International Journal of Geo-Information

MDPI

Article

Multi-Aspect Analysis of Object-Oriented Landslide Detection Based on an Extended Set of LiDAR-Derived Terrain Features

Kamila Pawłuszek [1,*], Sylwia Marczak [1], Andrzej Borkowski [1] and Paolo Tarolli [2]

[1] Institute of Geodesy and Geoinformatics, Wrocław University of Environmental and Life Sciences, 50-375 Wrocław, Poland

[2] Department of Land, Environment, Agriculture and Forestry, University of Padova, Agripolis, viale dell'Università 16, – 35020 Legnaro (PD), Italy

* Correspondence: kamila.pawluszek@upwr.edu.pl

Received: 10 May 2019; Accepted: 20 July 2019; Published: 24 July 2019

Abstract: Landslide identification is a fundamental step enabling the assessment of landslide susceptibility and determining the associated risks. Landslide identification by conventional methods is often time-consuming, therefore alternative techniques, including automatic approaches based on remote sensing data, have captured the interest among researchers in recent decades. By providing a highly detailed digital elevation model (DEM), airborne laser scanning (LiDAR) allows effective landslide identification, especially in forested areas. In the present study, object-based image analysis (OBIA) was applied to landslide detection by utilizing LiDAR-derived data. In contrast to previous investigations, our analysis was performed on forested and agricultural areas, where cultivation pressure has degraded specific landslide geomorphology. A diverse variety of aspects that influence OBIA accuracy in landslide detection have been considered: DEM resolution, segmentation scale, and feature selection. Finally, using DEM delivered layers and OBIA, landslide was identified with an overall accuracy (OA) of 85% and a kappa index (KIA) equal to 0.60, which illustrates the effectiveness of the proposed approach. In the end, a field investigation was performed in order to evaluate the results achieved by applying an automatic OBIA approach. The advantages and challenges of automatic approaches for landslide identification for various land use were also discussed. Final remarks underline that effective landslide detection in forested areas could be achieved while this is still challenging in agricultural areas.

Keywords: landslide detection; OBIA; segmentation; DEM; LiDAR

1. Introduction

A landslide is a movement of a mass of rocks, debris, or earth down a slope [1]. This natural hazard can lead to severe consequences such as economic and infrastructure damage and human casualties [2].

To mitigate the negative effects of landslide occurrence, an effective risk assessment is unavoidable [3]. Landslide identification in a specific study area is a fundamental step, which enables an assessment of landslide susceptibility and the associated risk [3–5]. Landslide identification can be carried out using a variety of techniques, which are mainly divided into conventional and remote sensing techniques [6,7]. The conventional methods mainly comprise geomorphological field mapping, aerial photo interpretation and surface and subsurface monitoring, which make these methods often time-consuming [7]. Moreover, landslide detection is extremely challenging and, sometimes, even unachievable, particularly in mountainous areas covered by dense vegetation [8,9]. Recently, remote sensing technologies have increased in importance and they are mainly focused on

data delivered by synthetic aperture radar (SAR), high resolution multi-spectral images [10] and digital elevation models (DEMs) obtained from space or airborne sensors [3,11–13].

Among these, airborne laser scanning (LiDAR) provides highly detailed DEM, thus out-performing traditional surveying techniques [14]. Analysis of DEM facilitates conventional methods as well as accelerates the development of automated approaches for landslide detection, especially in mountainous areas where accessibility is problematic. Moreover, due to the ability to penetrate vegetation, it is also possible to generate a highly detailed DEM in forested areas [15]. Landslide detection using detailed DEM can be performed using a pixel-based approach (PBA), which is based on the analysis of individual pixel values, which are then classified into the corresponding classes [16]. An alternative and relatively recent method, which out-performs PBA, is an object based image analysis (OBIA) [17,18]. OBIA uses the properties of image objects, derived from the segmentation process, for their subsequent classification [19].

There are several examples of OBIA applications for landslide identification using optical remote sensing data. However, there are only a few that investigate the application of OBIA to landslide detection by only utilizing DEM data and its derivatives. Martha et al. [20] utilized 5.8 m multispectral data (from Resourcesat-1) and a 10 m DEM (generated from 2.5m Cartosat-1 imagery) for landslide identification in the rugged Himalayas in India. DEM-derivatives such as slope, terrain curvature, hillshade, and flow direction, along with the DEM and normalized difference vegetation index (NDVI) were used as input layers for OBIA. Five landslide types were detected by this method with 76.4% recognition and 69.1% classification accuracies. Seijmonsbergen et al. [21] applied multi-temporal LiDAR derived DEMs for geomorphological change analysis in western Austria. DEM-derived layers such as the slope angle layer, an elevation percentile layer and two topographic openness layers (with kernel sizes of 25 m and 250 m) together with multi-temporal, ortho-rectified, panchromatic, color, and infrared aerial photos, have been applied to stratified OBIA classification. This allows for the mapping of six geomorphological features with an overall accuracy of 84%. Van Den Eeckhaut et al. [9] carried out the OBIA by using only DEM. They utilized DEM-derivatives such as mean and standard deviation of slope, curvature, roughness, openness, and Sky-View factor (SVF). This approach comprised two stages: Firstly, after segmentation, large agricultural fields and potential landslides were identified; secondly, two more classes were distinguished, such as landslide bodies and other areas. The overall accuracy of this approach is approximately 70% for a landslide body while in the case of identifying only the main scarps, the accuracy increased to 90%. Li et al. [17] utilized only DEM-derivatives such as DEM, slope, aspect, and surface roughness and their textural features. After feature selection, they resign from texture-related features, which suggested that they might be of little use. Then, using the selected variables and random forest (RF) and support vector machine (SVM) classification, automatic landslide identification was performed and overall accuracy of 77.36% for the RF algorithm and 76.87% for the SVM algorithm was achieved.

Our work was inspired by two studies given by Van Den Eeckhaut et al. [9] and Li et al. [17], which present an application of OBIA and DEM data for forested landslide detection. Automatic landslide detection methods benefit from the uniqueness of landslide geomorphology (characteristic roughness and landslide features such as main and minor scarps, crack, etc.). However, for rural areas, typical landslide features can be degraded, or even vanished, due to direct or surrounding agricultural activities. Therefore, having considered these issues, an open question remains to be explored: Based on DEM derivatives only, what OBIA approach is scalable to various land cover conditions? This research is an attempt to answer this question. We have applied the OBIA approach to areas with different land cover. We test OBIA scalability on the heavily agricultural and vegetated areas in the Polish Carpathians. We discuss the opportunities and challenges of automatic approaches under diverse land cover conditions. An additional objective of our research is to analyze various aspects influencing OBIA performance in the context of automatic landslide detection. More specifically, we analyze the potential of additional DEM derivative layers and performed texture analysis in the context of OBIA enrichment. Another novel aspect of this study is the investigation of OBIA performance depending on DEM resolution.

2. Study Area

The study area was located in the central part of the Outer Carpathians (in the Małopolskie municipality, Poland), close to Rożnów Lake (Figure 1), and covered latitudes 49°43'N to 49°46' N and longitudes 20°38' E to 20°43' E. Most of the study area consisted of agricultural land (42%), while forests accounted for 34% of the total area [22]. Despite the existence of landslides and landslide-prone areas, the affected areas were still extensively used for economic purposes [22]. The broad analysis of landslide density in various land use classes for the presented study area can be found in Kroh [22]. Landslide identification is challenging due to extensive land management, in the form of farmland, grasslands, and pasture, and continuous development of constructions in this area (Figure 2).

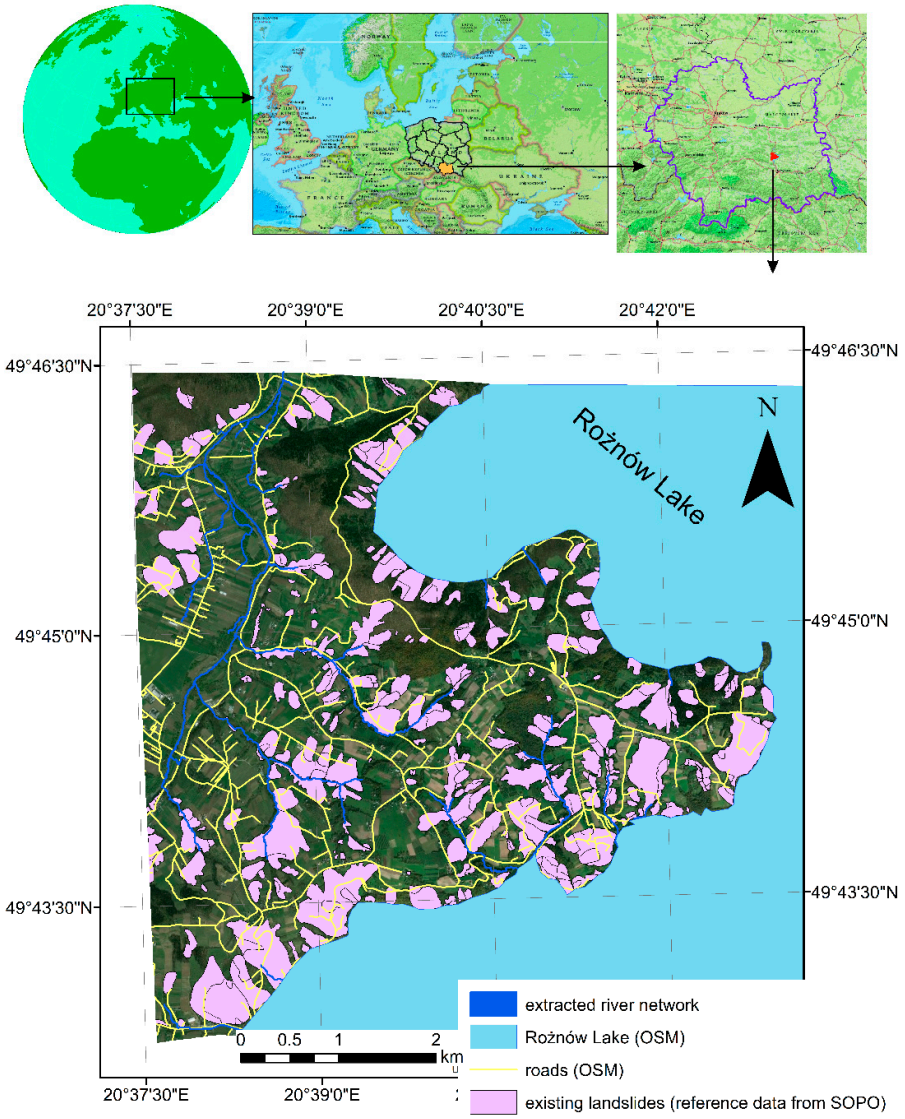

Figure 1. Study area location within Poland and existing landslides overlap to an RGB orthophoto. Landslides are obtained from the National landslide database (SOPO) and additional auxiliary data.

Figure 2. Perspective view of the study area, captured during the field investigation.

From a geological point of view, our study area is located in an area of allochthones mantle built up mainly from flysch deposits [22–25]. Flysch deposits (i.e., clearly stratified rock series consisting of numerous and alternately arranged layers of sandstones, siltstones, and shales, with rare layers of conglomerates, marls, or limestone) generate very favorable conditions for landslide occurrence [3,8,24,25]. An alternating arrangement of permeable and impermeable materials implies a greater landslide occurrence probability. Additionally, the Łososina River flows through the study area and this is the left tributary of the Dunajec River, which is a mountainous river with a rocky and stony bottom, characterized by short-term and significant water surges [23]. During these surges, water undercuts the slope, causing landslides [23,25]. This can be clearly observed in Figure 1, where landslides are mostly located close to the Rożnów Lake or river valleys. Another factor causing landslides within the study area is the infiltration of rainwater, which results in water accumulation and increases pore water pressure. This reduces the soil strength and increases stress, abrasion, and erosion [23,25].

3. Data

In this study, three datasets were used: A landslide inventory map from the Polish Geological Institute database (Section 3.1), LiDAR data (Section 3.2; which allowed us to derive a high resolution DEM) and the Open Street Map database (roads, Section 3.3.1 and river and streams, Section 3.3.2).

3.1. Landslide Inventory Map

The Carpathian Division of the Polish Geological Institute developed a Landslide Counteracting System, called SOPO (http://geoportal.pgi.gov.pl/portal/page/portal/SOPO/ Wyszukaj3). The SOPO project mainly aims to develop and deliver geological data and information about landslide locations and areas prone to mass movements in Poland. These maps provide significant information for spatial planning and management institutions [3,13,23,25] and help them to avoid landslide-endangered areas when planning building and infrastructure development. SOPO aims minimizing potential losses resulting from landslide activity [22,25].

Existing landslide-related information within the SOPO database was acquired using conventional techniques, mostly using field reconnaissance, visual interpretation of aerial photographs and analysis of historical data. Landslide identification over the study area was carried out in 2010 to 2011 [25,26]. The investigation covered an area of 26 km^2, of which 6.72 km^2 are affected by landslides. This means that landslides occupy almost 25% of the entire study area. 372 landslides were identified with areas ranging from 500 m^2 to almost 3000 m^2 [25,26]. Following Vernes [27] updated classification provided by Hungr et al. [28], landslides within the study area are represented

by rock rotational, clay/silt rotational, planar, and compound slides, which are slow to very slow-moving. Slides are mostly located on the slopes of valleys and water reservoirs and places where backward erosion increases slope failure, such as areas around roads and rivers [23,25].

3.2. LiDAR Data

LiDAR data were collected in the framework of the Country's Protection System, called the ISOK project (http://www.isok.gov.pl). Point clouds were captured using the Riegl LiteMapper 6800i system, based on the Q680i laser scanner in the year 2012. The planimetric density of the point cloud is 4 to 6 points per square meter and the estimated RMSE for the height component is approximately 0.15 m [29]. After the point cloud filtering, the final DEM (representing bare earth topography) was generated at a resolution of 0.5 m [13].

3.3. Auxiliary Data

We used auxiliary data for the segmentation step because landslides are mostly located on the natural slopes of valleys and places where backward erosion increases landfalls, such as areas around roads and rivers. For a better representation of landslide object geometry (especially in the case of the landslide foot located close to rivers or roads) road and river layers were included into the segmentation process. However, this process does not affect landslides located far from roads or rivers. In these cases, the segmentation was performed without consideration of auxiliary data.

3.3.1. Road Network

The road layer was captured by the OpenStreetMap platform, which is a free map service that provides vector data for the whole world. The road network acquired by OSM has been updated at various times and the oldest update was recorded in 2012. The acquired data was visually validated using satellite imagery available on Google Earth and a good match with the contours represented on the DEM was observed. Based on visual evaluation, OSM road data represents all paved roads. Small dirt roads were not been included in this data. Many researchers stated that the high road density in mountainous areas increases the probability of landslide activation [3,9,30–34]. The main reason for this is that roads may redistribute and concentrate surface water flow, undercut the slopes, and break the rock structures and, therefore, decrease the slope stability [35]. The road network within the study area was very dense (Figure 1); therefore, for a precise segmentation process, the road network was utilized.

3.3.2. Generation of Accurate River and Stream Networks

Based on visual inspection of satellite data in Google Earth and shaded DEM, many small rivers and streams were observed within the study area, which were not presented on OSM. Since the OSM rivers layer contained only the Lososina River and Rożnów Lake, we decided to extract a more complete river network by calculating the flow direction and flow accumulation from the DEM. Since river network extraction was not a goal of the research and this was only used for better representation of the segmented object in the conceptual term, we decided to extract this network by calculating the flow direction and flow accumulation by using only DEM. To identify streams and watercourses, we performed classification of flow accumulation values. This classification was carried out using natural breaks method. Six classes were classified where the first three classes with the highest values were considered to be the best for river and watercourse extraction. This threshold was suitable enough to digitally represent the rivers, based on visual interpretation. Data from rivers and streams are considered to be helpful in the segmentation process, where landslides usually border the rivers or streams [9]. All analyses performed within this subsection were performed using ArcGIS.

4. Methodology

The overall methodology is presented in Figure 3 while landslide detection using OBIA is presented in Figure 4. Besides landslide detection, significance analysis of the different aspects influencing OBIA was also analyzed. This was performed by comparing accuracy indexes from various strategies (which involve various data and parameters). The starting point for further investigation was the generation of the DEM. Since our study aimed, inter alia, at determining the impact of the DEM resolution on the accuracy of the OBIA classification, DEMs with a resolution of 1 m up to 10 m were created by resampling original DEM with the majority of elevation values. Then the river's pixels were excluded from the reference data by applying the previously extracted, precise rivers and streams network. All analyses were performed using ArcGIS and eCognition software.

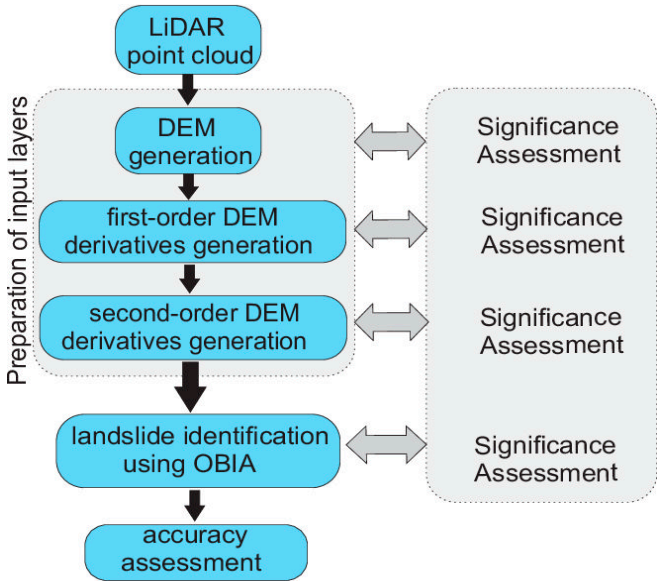

Figure 3. Overall methodology flowchart. Landslide identification using object-based image analysis (OBIA) was performed after preparation of input layer and significance assessment of various aspects. Detailed OBIA methodology is presented in Figure 4.

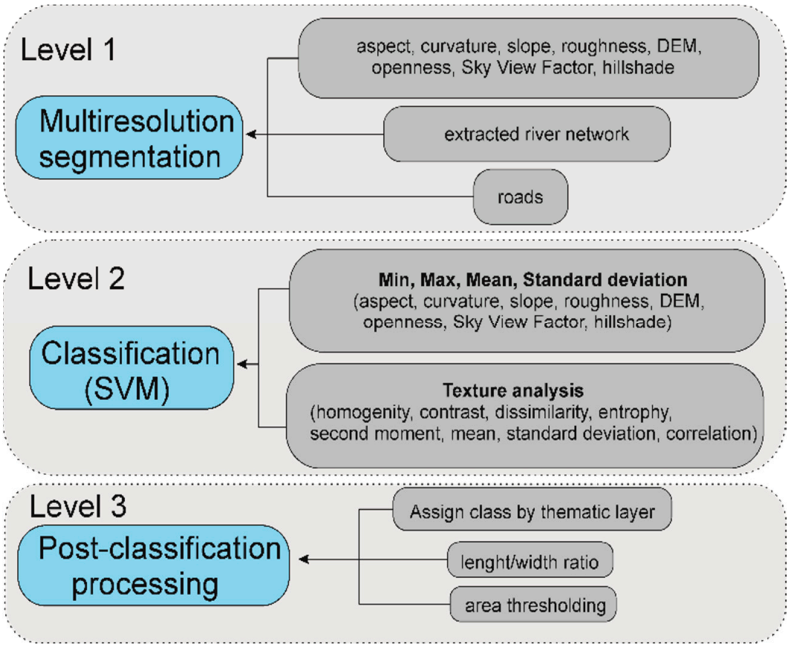

Figure 4. Detailed OBIA methodology divided into three crucial levels.

4.1. Generation of First and Second-order DEM-derivatives

Slope was considered as a direct indicator of landslides. Its exposition (aspect) can also influence landslide creation [3]. Openness as the difference between original DEM and smoothed DEM presents residual topography, which reflects landslide characteristic signatures [9,13]. Similarly, curvature represents concavity and convexity and can indicate the main scarp, which is concave in its geometry [3]. In [13], roughness, openness, and curvature and in [9] slope, aspect, curvature, roughness, openness, and the Sky-View factor (SVF) have been considered as important variables for landslide detection. Li et al. [17] also considered slope, aspect, and texture layers as useful for landslide detection. According to previous findings [5,13,36], a hillshade layer is especially informative for landslide detection, therefore, it was used in this research [13,36]. The above mentioned topographical layers are currently widely applied in various landslide-related studies, therefore broad descriptions of these layers is presented in [3,5,9,13,17,36]. Based on previous experiences aspect, curvature, slope roughness, openness, SVF, hillshade, and DEM were also used in this study. ArcGIS software and Relief Visualization Toolbox were applied for calculation of these derivatives. Size of the calculation matrix was selected based on [13]. Due to the space limitation, a graphical representation of this DEM-derivatives and its relation to landslides can be found in our previous studies in [3,13,36]. According to previous findings [13,36], a hillshade layer was also used in this investigation. It was decided to call them first-order DEM-derivatives because they are diverse mathematical computations of DEM. Since textural features consider the spatial relationship between pixels [17,37], the layers of entropy, correlation, angular second moment, homogeneity, contrast, and dissimilarity were implemented. These layers have been called second-order DEM-derivatives, because they were calculated from first-order DEM-derivatives. Each second-order layer (entropy, homogeneity, etc.) was calculated from all first-order DEM derivatives. Specifically, entropy was calculated from slope, DEM, aspect, etc. This provides a total of 64 layers (eight first-order multiplied by eight second-order layers). These measures of textural image features are defined, inter alia, in [17,37]. Moreover, after the segmentation process also the minimum, maximum, mean, and standard deviation were calculated for each segmented object and all DEM derivatives. These second-order DEM-derivatives were calculated using eCognition software.

4.2. Classification Using OBIA

4.2.1. Segmentation

The general concept of OBIA classification is presented in Figure 4. It comprised of subsequent steps, namely multiresolution segmentation, classification, and post-processing. eCognition was considered to be the most suitable software for this purposes and was used for all of the steps described in this section. Multiresolution segmentation (MRS) is the widely used method for segmentation purposes [17]. It is a bottom-up segmentation based on a grouping technique. MRS uses region growing algorithms that, starting from individual pixels, connect the most similar neighboring regions, as long as the user-defined threshold factor of internal heterogeneity is not exceeded. The algorithm uses three parameters: Scale, shape weight, and compactness. For the MRS, first-order DEM derivatives and auxiliary data with the same weights were applied.

The selection of an appropriate scale is probably the most important step. The scale should consider the resolution of the input data used as well as the size and complexity of the landslides within the study area. To eliminate large agricultural fields and to find potential landslides, [9] applied, for 2 m DEM resolution, two scales equal to 13 and 35 representing object areas of 53 m^2 (13 × 4 m^2) and 140 m^2 (35 × 4 m^2). Li et al. [17] selected the scale parameter based on an iterative trial-and-error optimization method for the 3 m DEM resolution they visually selected the segmentation result with a scale value of 10, which is equivalent to an area of 90 m^2 (10 × 9 m^2). Similar to the aforementioned papers, in this study we also tested a wide range of scales, covering values from 10 up to 130. For 2 m DEM, it was found that the optimal scale parameter was between 20 and 40, which referred to an object area between 80 m^2 and 160 m^2. For the selection of scale parameters, the DEM resolution and desirable area of segmented object have to jointly be taken into account.

4.2.2. Training and Validation Dataset

For supervised classification, training samples are necessary. Stratified random sampling design suffers from the effects of spatial auto-correlation [37,38] and, therefore, can artificially influence identification results. To avoid such shortcomings, randomly selected landslides sample objects (SLS) and non-landslide sample objects (SNLS) were considered in this study. Table 1 presents statistics of selected training samples. Chen et al. [37] and Li et al. [17] utilized a lot of training data (50% of the landslide objects and non-landslide objects ≈ 11 km², when the study area covered 21.6 km²) and, thus, the results were very close to the reference polygons. In contrast, we tested whether using a smaller amount of training samples led to worse identification results. Therefore, based on Table 1, our training samples utilized around 20% of the total study area

Table 1. Training and validation dataset.

	Training Dataset (km²)	Validation Dataset (km²)	Total Dataset (km²)
Landslides	2.01	4.71	6.72
Non-landslides	3.11	16.17	19.28
Total	5.12	20.88	26.00

4.2.3. SVM Classification

After the segmentation and training sample selection from referenced data acquired from SOPO, supervised classification was performed. Minimum, maximum, standard deviation, and mean values of segmented objects were used from each DEM derivative layer and classified using SVM classification. Several publications demonstrated an effective performance of the support vector machine (SVM) classification when compared to other supervised classification methods [5,13]. The SVM classification searches for an optimal hyperplane that separates the two classes by maximizing the margin between the nearest class points; the points lying at the borders are called vector supports and the center of the margin is the optimal separating hyperplane. In the case where data were not linearly separable, data points were projected onto a higher dimensional space in which data points effectively became linearly separable. For this projection, implementation using kernel techniques is necessary [39]. The most popular type of kernel functions used in SVMs is radial basis functions. This type of kernel function was also used in this study. Other SVM parameters implemented in eCognition were used as defaults.

4.3. Various Strategies of OBIA Classification Used for Multi-Aspect Significance Assessment

Based on Figure 3, we mainly analyzed four crucial aspects, which influence the performance of the OBIA classification. Specifically, we analyzed: (1) DEM resolution, (2) segmentation scale, (3) significance of DEM derivatives, and (4) how accuracy changes when particular DEM derivatives were subsequently added.

Having considered our previous work [5,13], the finest DEM resolution is not always the best choice. Therefore, we tested various DEM resolutions and their effect on OBIA performance. DEM resolution directly influences the selection of the scale, which is used for image segmentation, thus, we also tested this parameter. Finally, we also assessed the significance of each DEM-derivative in landslide detection using OBIA. This was performed via many single-layer OBIA classifications and analysis of accuracy indexes (OA, KIA). This significance assessment was performed for first- and second-order DEM derivatives. Li et al. [17] revealed that second-order layers (texture) do not increase identification accuracy. Therefore, an additional goal of the present study was to verify this fact and to test the second-order features effectivity in another study area with different land uses. The studies that inspired us [9,17] were performed for forest areas only. Our investigation also covered agricultural areas.

Independently, we checked how the accuracy of the classification would subsequently change by adding each layer into the classification. As described in Section 4.1, second-order DEM derivatives were calculated from first-order DEM derivatives. Therefore, starting from the entropy

calculated from eight first-order DEM derivatives, an additional second-order layer calculated also from first-order layers was added subsequently. Finally, taking into account eight first-order DEM derivative and eight second-order derivatives, 64 layers were used (in the end of the Figure 6b.)

4.4. Post-Classification Processing and Accuracy Assessment

After significance assessment and selection of the most suitable DEM resolution, segmentation scale, and DEM-derivatives, the final landslide detection was performed by applying post-processing steps in order to refine the final results. The aim of the post-processing step is to remove false positive results from the classification results. Despite the fact that river pixels were removed from the training process, some false positive objects still appeared in the results. This is common in the river-beds or agricultural scarps, where geomorphology is very similar to the landslide. However, these false positives can be removed by applying post-processing algorithms. Four post-processing steps were applied in our investigations (Figure 4). Firstly, a tool named sign class by thematic layer within eCognition software was applied. This allowed us to group classify objects into one class with consideration of thematic layers. Secondly, by analyzing the geometry of landslides, it could be observed that they were characterized by consistent areas. The landslide objects are represented as closed objects without "holes" inside them. In GIS language these holes are called 'do-nut' holes, which usually need to be filled (some islands of pixels/objects, which were somehow not classified as landslides and they are not desirable). Therefore, closing geometry algorithms were used to exclude holes inside the detected landslide objects. Thirdly, by analyzing the geometry of the landslide segments it can be observed that landslide objects were not long and narrow (e.g., 1 m in width and 50 m in length), thus objects having such geometrical properties should be eliminated from the landslide class. To apply this, a length to width index was evaluated. Our result shows that elimination of objects whose length/width index was greater than 5 refined the detection results. This threshold was assessed based on a visual interpretation of randomly selected false positive objects, resulting from the OBIA classification. Moreover, it was noted that on the resulting classification map, there were a lot of objects with a very small area, not adjacent to other objects; they did not indicate the existence of landslides in those places. Therefore, the size of the landslides that existed in the studied area was investigated. Concerning reference data, the smallest landslide in this area covered an area of 500 m^2. Therefore, this value was set up as the threshold and landslide objects that were detected, which were smaller than this threshold were removed from the final landslide class. In the case of transferability to another study area, this threshold should be assessed according to the minimum landslide size in the given study area. However, it is post-processing that only refined the final results, thus, KIA was increased from 0.55 into 0.61 and OA was increased from 83.4% into 85.5%.

In order to assess the accuracy of the results, two indices were applied: Kappa index (KIA) and overall accuracy (OA). The OA shows the sum of correctly classified objects divided by the total object number. The Kappa index is extensively used in accuracy assessment of classifications [13,17,39]. The KIA measures the agreement between a classification and truth values. A kappa value of 1 represents perfect agreement, while a value of 0 represents no agreement. For accuracy assessment, we adopted these indices to measure the agreement between the results achieved and the reference data from SOPO database (validation dataset, see Section 4.2.2). eCognition was used in this work, for all steps described in this section.

5. Results

Besides the OBIA analysis, a significance analysis of first- and second-order DEM derivatives, DEM resolution and segmentation scale were evaluated. All of these analyses are presented in the following subsections.

5.1. DEM Derivatives Significance Assessment

The first step in methodology processing was to analyze the significance of the selected DEM derivatives. Based on Figure 5a it can be observed that OA and KIA values were quite similar for particular layers. The results indicated that the selection of first-order DEM derivatives was appropriate and each of them were relevant and provided valuable information for landslide detection processing. Based on OA and KIA values (Figure 5), slope, curvature, and hillshade layers were slightly more significant than other layers. Identification of a landslide using only the slope layer provided 72% of OA and KIA were equal to 0.30, while using the curvature layer, OA and KIA were equal to 72% and 0.28 was achieved, respectively. As was observed on Figure 5b, the second-order analysis of mean standard deviation and second moment had a KIA index and OA close to zero, while other layers had similar values of OA and KIA index.

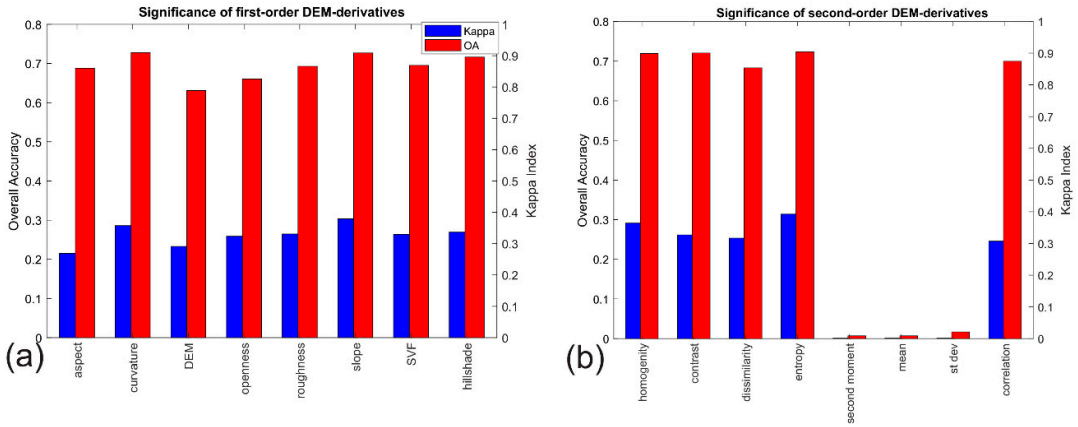

Figure 5. Digital elevation model (DEM)-derived layer significance assessment for (**a**) the first-order DEM-derivatives, and (**b**) second-order DEM-derivatives.

Based on the result provided by the significance assessment that was presented on Figure 5, particular DEM derivatives were subsequently added as an input dataset. Then classification was performed for a given stack of layers in order to evaluate the classification accuracy when using a given combination of input layers. Input layers were added successively in their order of decreasing significance. Figure 6a shows the accuracy increase when input layers (first-order derivatives) were successively added. It can be observed that by using more than four of the most significant layers, the accuracy of landslide identification did not increase significantly (the OA and KIA were almost stable). If the subsequently added layers were not ordered based on their significance, the subsequent OA and KIA could not adequately increase, however, ordering issues were not analyzed in this research.

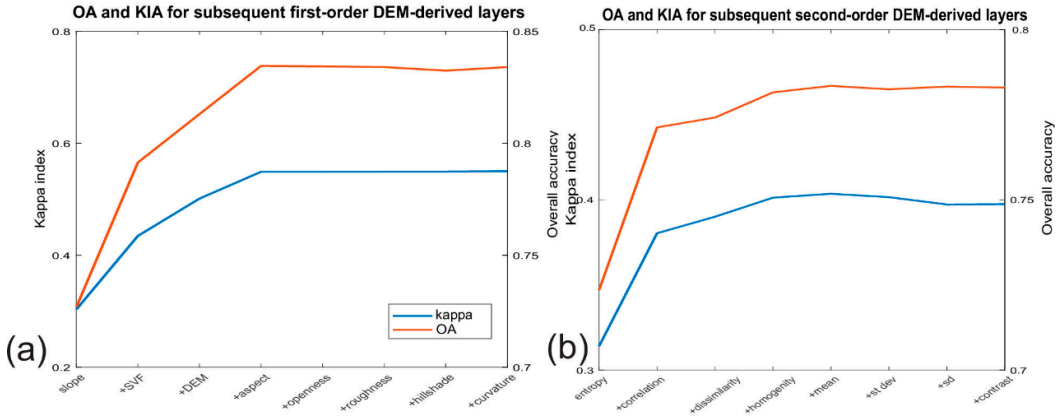

Figure 6. Kappa and accuracy in reference to subsequently added (**a**) first-order DEM-derived layers and (**b**) second-order DEM-derived layers.

In Figure 6b, the OA and KIA indices of subsequently added second-order DEM derivatives are presented. When analyzing Figure 6b it can be seen that the initial four second-order derivatives provided the bigger increase of accuracy. Based on this, it can be observed that a similar situation existed in both situations (the first- and the second-order DEM derivatives). Very small changes in OA and KIA were observed when a fifth and sixth layer was added to the input dataset. However, the KIA index and OA did not exceed 0.4 and 0.8, respectively. When comparing these results to the first-order derivatives (OA = 0.85 and KIA = 0.55), it could be concluded that better accuracy could be achieved with a first-order DEM derived layer, therefore the application of other, second-order layers was abandoned from further processing. Thus, only eight first-order DEM-derivatives were used for the significance assessment of DEM resolution, segmentation scale, and final landslide detected map generation.

5.2. Scale Significance and DEM Resolution Assessment

After evaluation of the input DEM derivative layers, the scale size was evaluated. It can be observed that with increasing scale, OA and KIA decreased rapidly when the scale was greater than 40.

For the scale equal to 20, significance of DEM resolution was also evaluated and presented in Figure 7b. It can be seen that the classification accuracy for data with a resolution between 2 m and 5 m remained stable. The highest OA value was recorded for the 2 m × 2 m dataset (OA = 0.8340), while the highest KIA was obtained for the 5 m × 5 m data (KIA = 0.5541). The accuracy of the classification using a resolution above 5 m was clearly degraded.

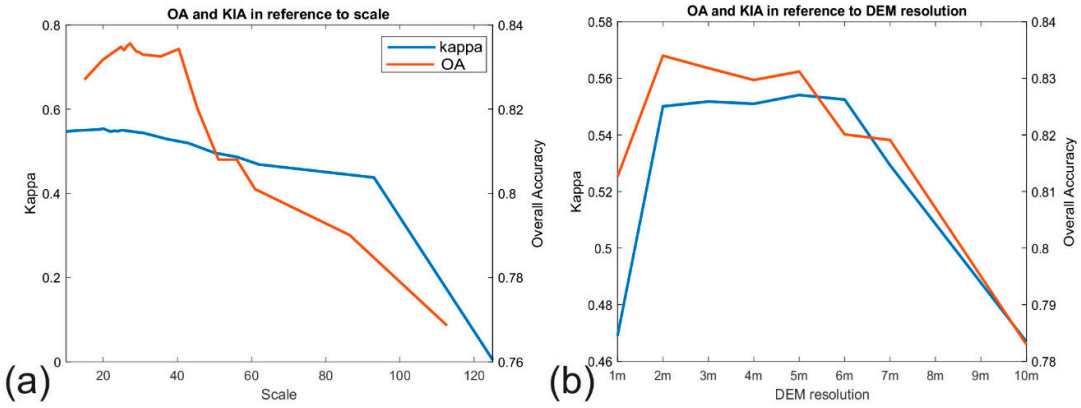

Figure 7. Kappa and accuracy with reference to (**a**) scale and (**b**) DEM resolution used for segmentation in OBIA.

5.3. Post-Processing and Final OBIA-Derived Landslide Map Generation

After the classification step, post-processing algorithms were applied in order to achieve a final map showing the detected landslides. For first-order DEM-derivatives, four steps were performed, including assigning class by thematic layer, object closing, thresholding of length/width index, and minimum object analysis. As a thematic layer, we used the river and road network. A final landslide map was generated by means of OBIA, 2 m DEM, first-order DEM-derivatives, and post-processing with OA and KIA equal to 85.50% and 0.6, respectively (Figure 8 and Table 2).

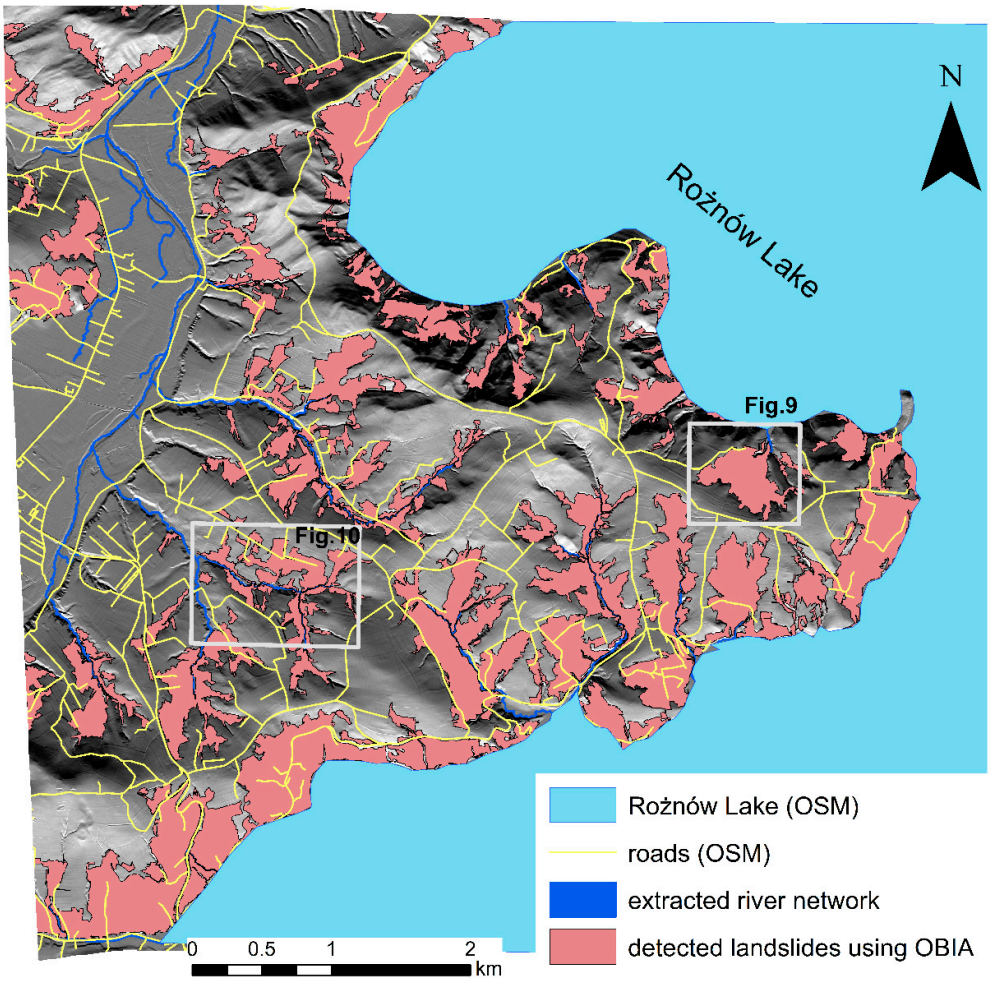

Figure 8. Final map of the detected landslides using OBIA.

Table 2. Accuracy assessment (confusion matrix) of the final landslide map.

	No Landslide Objects	Landslide Objects
Producer Accuracy	0.89	0.71
User Accuracy	0.91	0.67
KIA	0.58	0.61

6. Discussion

Discussion of the results described can be divided into four subsections: Section 6.1—DEM derivative significance, Section 6.2—segmentation scale and DEM resolution, Section 6.3—capabilities and limitations of automatic approaches, and Section 6.4—OBIA versus PBA.

6.1. DEM Derivative Significance

Among the tested DEM derivatives, first-order DEM derivatives (such as slope, aspect, curvature, hillshade, openness, SVF, and roughness) provide useful topographical information for automatic identification of landslides. Furthermore, our results showed that using more than four input first-order derivatives did not significantly increase classification accuracy. Thus, these layers could be omitted in cases where input layers are limited.

Second-order DEM derived layers (texture layers) were significantly less useful for automatic landslide identification than first-order DEM derived layers because they did not provide effective information, retrievable by OBIA. Moreover, the application of second-order features was more time consuming, especially in the classification training process [17] confirmed that second-order features are of less use.

6.2. Segmentation Scale and DEM Resolution

The authors of previous studies [13] found that high resolution DEM was not effective for automatic landslide mapping using PBA. In the our investigations, we found that OBIA was not sensitive to the DEM resolution used and it was found that the resolutions between 2 m and 5 m achieved the best accuracy of automatic landslide detection using OBIA. The accuracy of the classification using a resolution above 5 m was clearly degraded. This is mostly contributed to the loss of details in the DEM and characteristic landslide morphology cannot be represented on such a coarse DEM. Scale is a very important parameter for the segmentation process. For 2 m DEM, it was found that the optimal scale parameter was between 20 and 40. It is worth considering that the segmentation scale is directly related to the DEM resolution used. For a segmentation scale equal to 25, DEM resolution between 2 m and 5 m provided the best results. Thus, in order to select an appropriate segmentation scale and DEM resolution, both aspects have to be jointly examined. Therefore, for effective consideration, the area of segments should be used. The best accuracy was demonstrated for an object covering an area of approximately 100 m^2. This value depends on the landslide size within the study area. However, similar areas of segmented object equal to 90 m^2 were reported as also being effective by other authors [9,17]. Choosing the right scale is currently the subject of many studies, as it is a very challenging issue. It is difficult to determine a method that would mathematically select appropriate scale for the specific study area.

6.3. Capabilities and Limitations of Automatic Approaches

Kroh et al. [22] reported that there are no land changes within the study area, resulting from landslide activity. Around 34% of the study area is covered by forest and 40% is covered by agriculture. Landslides within the study area are slow and very slow forming, therefore their activity does not imply a loss of vegetation. Simultaneously, human activity (e.g., agriculture) smooths or even erases typical landslide features, which makes landslide identification extremely challenging. Despite the achievements of OA and KIA index, it is worth highlighting the complexity and challenges of automatic approaches for landslide identification. These approaches can be effectively applied in forested areas, where the morphology of the terrain has not been greatly altered by human activities. In Figure 9, detection of the landslides covered by forest is presented. Green areas represent the existing landslide database and pink areas represent landslides detected by means of our presented approach. This picture underlines the performance of the automatic approach. Based on the reference data provided by conventional methods, two diverse landslides were mapped (Figure 9d). However, the automatic approach using OBIA identified the area as being one landslide (Figure 9c). Visual interpretation of the DEM derivatives showed that it is, in fact, one landslide. The imprecise identification is probably connected to limited terrain visibility in the forested areas as well as the unavailability of high-resolution DEM data during the landslide investigation.

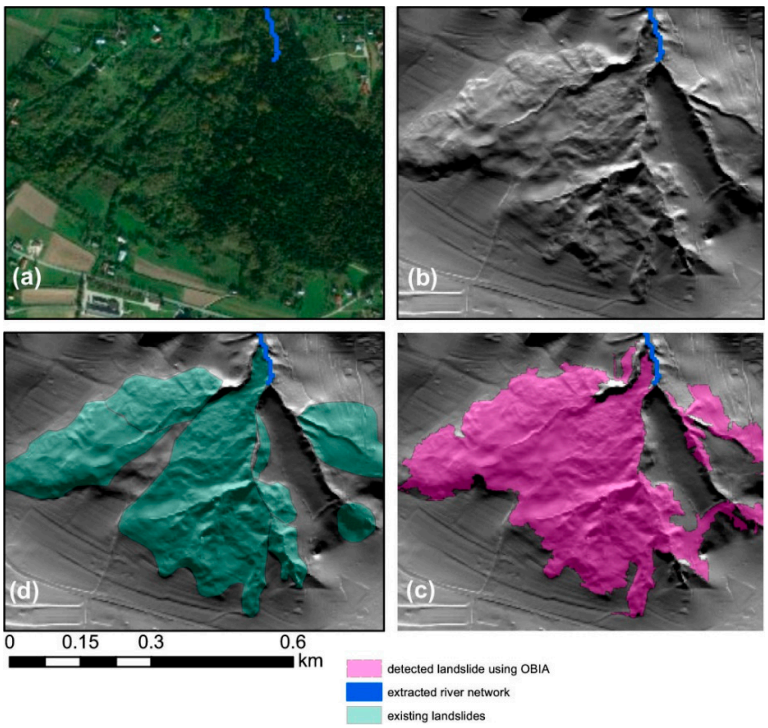

Figure 9. OBIA results in cases of forested areas: (**a**) Ortophoto, (**b**) shaded DEM, (**c**) landslide detected using OBIA, and (**d**) existing landslide in SOPO database.

On the contrary, where landslide vanishing factors appear, it is very challenging and even impossible to precisely detect landslides using automatic approaches. Figure 10 presents an example that demonstrated the limitations of the automatic OBIA approach. In this case, the morphology was changed by agricultural activities, as well as natural processes such as denudation etc. In such a case, topographic information, provided by DEM alone, was insufficient to detect landslides efficiently. In the present study, OBIA was not able to detect the landslide completely (see Figure 10c).

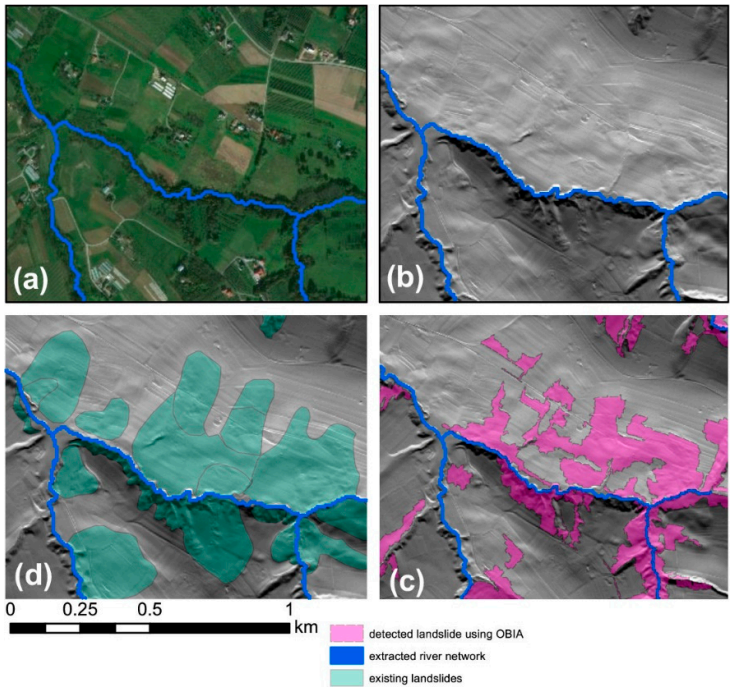

Figure 10. OBIA in agricultural areas: (**a**) Ortophoto, (**b**) shaded DEM, (**c**) landslide detected using OBIA, and (**d**) existing landslide in SOPO database.

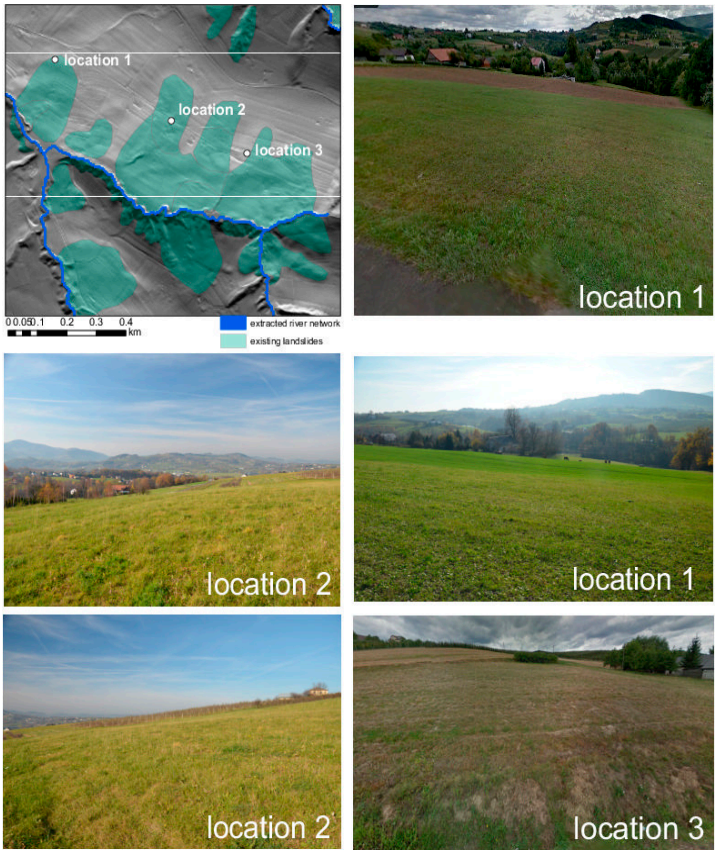

Figure 11. Challenges of automatic landslide detection in agricultural areas.

Landslide images taken during field reconnaissance are presented in Figure 11. It could be observed that land cultivation changes the topography significantly. Even during fieldwork, it can be very difficult to distinguish landslide areas from non-landslide areas.

6.4. OBIA versus PBA

PBA for automatic landslide identification in this study area was examined in depth during our previous research work [13]. The same study area, input data, SVM classifier but various approaches or units (pixels/objects) were used in this research and in [13]. The last one utilizes pixels while this paper utilized objects. Based on the results obtained within this work and the aforementioned paper, it can be stated that OBIA provides better accuracy than PBA. Comparing these two approaches for 5 m DEM resolution and SVM classification, the KIA index was 0.237 and 0.5541 for PBA and OBIA, respectively. This means that OBIA out-performed PBA. A similar conclusion was also presented by [17]. Moreover, when comparing our results with those achieved in the aforementioned paper, OBIA shows poor sensitivity to the selected DEM resolution while PBA was very sensitive to the selected DEM resolution. From another perspective, PBA could also achieve favorable results (KIA = 0.55), largely by using a coarser DEM resolution. The probable explanation for this is that PBA is based on individual pixels and very fine DEM resolution provides noisy results. OBIA is based on segments, therefore the results were more consistent. Contrary to PBA, OBIA demonstrated the best accuracy for DEM resolution between 2 and 5 m.

7. Conclusions

This research investigated OBIA applicability and performance for landslide identification, based on DEM data obtained from LiDAR in a study area of flysch deposits in the Polish Carpathians. Application of an experimentally defined set of rules allowed for effective landslide detection. The methodology was tested in an area affected by more than 370 landslides [25,26]. The identification procedure included (1) the preparation of DEM derivatives, (2) multi-resolution segmentation, (3) classification using SVM, and (4) post-processing classification refinement. Besides landslide identification, the diverse aspects influencing this approach (such as DEM resolution, segmentation scale, and the selection of DEM-derived input layers) were analyzed.

Based on a sensitivity analysis, the following features were chosen for the OBIA: Mean, standard deviation, minimum, and maximum of eight prepared DEM-derivatives, i.e., DEM, aspect, slope, curvature, roughness, openness, Sky-View factor, and hillshade. The multi-stage feature selection allowed for the exclusion of textural features because they did not improve the final accuracy but significantly extended the algorithm's working time.

Furthermore, other findings showed that OBIA was not sensitive to the resolution used however, a resolution between 2 m and 5 m allowed for the best accuracy in landslide identification. On the other hand, the results showed that the scale was also a very crucial parameter for OBIA applications in landslide detection. In this perspective, for a 2 m DEM resolution and a scale between 20 and 40, OBIA provided outstanding results.

By comparing our results with those from previous research studies [13] it was concluded that OBIA performed better than PBA for the same study area, under the same DEM resolution and classifier used.

In summary, the presented algorithm effectively identified landslide areas with an OA of 85% and a KIA of 0.60, revealing the potential of OBIA in landslide identification, especially in forested and agricultural areas.

Author Contributions: Conceptualization and supervision Kamila Pawłuszek, Andrzej Borkowski, Paolo Tarolli. Data captured and methodology have been provided by Kamila Pawłuszek and Andrzej Borkowski. Formal analysis and validation have been performed by Sylwia Marczak. Writing and Original Draft Preparation and results visualization have been done by Kamila Pawłuszek Review & Editing have been provided by Kamila Pawłuszek, Andrzej Borkowski, Paolo Tarolli.

Funding: This research has been supported by National Science Centre of Poland (Grant No. 2017/25/N/ST10/02365).

Conflicts of Interest: The authors declare no conflict of interest

References

1. Cruden, D.M. A simple definition of a landslide. *Bull. Eng. Geol. Environ.* **1991**, *43*, 27–29.
2. Leshchinsky, B.A.; Olsen, M.J.; Tanyu, B.F. Contour Connection Method for automated identification and classification of landslide deposits. *Comput. Geosci.* **2015**, *74*, 27–38, doi:10.1016/j.cageo.2014.10.007.
3. Pawłuszek, K.; Borkowski, A. Impact of DEM-derived factors and analytical hierarchy process on landslide susceptibility mapping in the region of Rożnów Lake, Poland. *Nat. Hazards* **2017,** *86*, 919–952, doi:10.1007/s11069-016-2725-y.
4. Highland, L.M.; Bobrovsky, P. *The Landslide Handbook a Guide to Understanding Landslides*; USA Geological Survey: Reston, Virginia, USA, 2008; pp. 34–39.
5. Pawłuszek, K.; Borkowski, A.; Tarolli, P. Towards the optimal pixel size of DEM for automatic mapping of landslide areas. *Int. Arch. Photogramm. Remote Sens. Spat. Inf. Sci.* **2017**, *42*, doi:10.5194/isprs-archives-XLII-1-W1-83-2017.
6. Ardizzone, F.; Cardinali, M.; Galli, M.; Guzzetti, F.; Reichenbach, P. Identification and mapping of recent rainfall-induced landslides using elevation data collected by airborne Lidar. *Nat. Hazards Earth Syst. Sci.* **2007**, 637–650, doi:isprs-archives-XLII-1-W1-83-2017.
7. Guzzetti, F.; Mondini, A.C.; Cardinali, M.; Fiorucci, F.; Santangelo, M.; Chang, K.T. Landslide inventory maps: New tools for an old problem. *Earth-Sci. Rev*. **2012,** *112*, 42–66, doi:10.1016/j.earscirev.2012.02.001.

8. Borkowski, A.; Perski, Z.; Wojciechowski, T.; Jozkow, G.; Wojcik, A. Landslides mapping in Roznow Lake vicinity, Poland using airborne laser scanning data. *Acta Geodyn. Geromater*. **2011**, *8*, 325–333.
9. Den, V.; Eeckhaut, M.; Kerle, N.; Poesen, J.; Hervás, J. Object-oriented identification of forested landslides with derivatives of single pulse LiDAR data. *Geomorphology* **2012**, *173*, 30–42, doi:10.1016/j.geomorph.2012.05.024.
10. Cheng, K.S.; Wei, C.; Chang, S.C. Locating landslides using multi-temporal satellite images. *Adv. Space Res*. **2004**, *33*, 296–301, doi:10.1016/S0273-1177(03)00471-X.
11. McKean, J.; Roering, J. Objective landslide detection and surface morphology mapping using high-resolution airborne laser altimetry. *Geomorphology* **2004,** *57*, 331–351, doi:10.1016/S0169-555X(03)00164-8.
12. Booth, A.M.; Roering, J.J.; Perron, J.T. Automated landslide mapping using spectral analysis and high-resolution topographic data: Puget Sound lowlands, Washington, and Portland Hills, Oregon. *Geomorphology* **2009**, *109*, 132–147, doi:10.1016/S0169-555X(03)00164-8.
13. Pawłuszek, K.; Borkowski, A.; Tarolli, P. Sensitivity analysis of automatic landslide mapping: Numerical experiments towards the best solution. *Landslides* **2018**, *15*, 1851–1865, doi:10.1007/s10346-018-0986-0.
14. Tarolli, P. High-resolution topography for understanding Earth surface processes: Opportunities and challenges. *Geomorphology* **2014**, *216*, 295–312, doi:10.1016/j.geomorph.2014.03.008.
15. Wojciechowski, T.; Borkowski, A.; Perski, Z.; Wójcik, A. Dane lotniczego skaningu laserowego w badaniu osuwisk przykład osuwiska w Zbyszycach (Karpaty zewnętrzne). *Przegląd Geologiczny* **2012**, *60*, 1–8. (In Polish).
16. Rosenfeld, A. *Segmentation: Pixel-Based Methods. In Fundamentals in Computer Vision 225–238*; Cambridge University Press: Cambridge, UK, 1983.
17. Li, X.; Cheng, X.; Chen, W.; Chen, G.; Liu, S. Identification of forested landslides using LiDar data, object-based image analysis, and machine learning algorithms. *Remote Sens*. **2015**, *7*, 9705–9726, doi:10.3390/rs70809705.
18. Keyport, R.N.; Oommen, T.; Martha, T.R.; Sajinkumar, K.S.; Gierke, J.S. A comparative analysis of pixel- and object-based detection of landslides from very high-resolution images. *Int. J. Appl. Earth Observ. Geoinf.* **2018**, *64*, 1–11, doi:10.1016/j.jag.2017.08.015.
19. Blaschke, T. Object based image analysis for remote sensing. *ISPRS J. Photogramme. Remote Sens*. **2010**, *65*, 2–16, doi:10.1016/j.isprsjprs.2009.06.004.
20. Martha, T.R.; Kerle, N.; Westen, C.J.; Jetten, V.; Kumar, K.V. Segment optimization and data-driven thresholding for knowledge-based landslide detection by object-based image analysis. *IEEE Trans. Geosci. Remote Sens*. **2011**, *49*, 4928–4943.
21. Seijmonsbergen, A.C.; Anders, N.S.; Bouten, W. Geomorphological Change Detection Using Object-Based Feature Extraction from Multi-Temporal Lidar Data. *IEEE Geosci. Remote Sens. Lett.* **2013**, *10*, 1587–1591.
22. Kroh, P. Analysis of land use in landslide affected areas along the Łososina Dolna Commune, the Outer Carpathians, Poland. *Geomat. Nat. Hazards Risk* **2017**, *8*, doi:10.1080/19475705.2016.1271833.
23. Gorczyca, E. Morphodynamics of the River Łososina Channel after an extreme flood (Western Carpathian Mountains). *Geografija* **2007**, *43*, 8–15.
24. Perski, Z.; Wojciechowski, T.; Borkowski, A. Persistent scatterer SAR interferometry applications on landslides in Carpathians (Southern Poland*). Acta Geodyn. Geomater.* **2010**, *7*, 1–7.
25. Gorczyca, E.; Wrońska-Wałach, D. Objaśnienia do Mapy osuwisk i terenów zagrożonych ruchami masowymi w skali 1:10000, gm. Łososina Dolna, pow.: Nowosądecki, woj: Małopolskie. Available online: http://mapa.osuwiska.pgi.gov.pl (accessed on 5 June 2018) (In Polish).
26. Bąk, M.; Długosz, M.; Gorczyca, E.; Kasina, K.; Kozioł, T.; Wrońska-Wałach, D.; Wyderski P. Mapa osuwisk i terenów zagrożonych ruchami masowymi w skali 1:10000, gm. Łososina Dolna, pow. nowosądecki, woj. Małopolskie. Available online: http://mapa.osuwiska.pgi.gov.pl (accessed on 5 June 2018) (In Polish)
27. Varnes, D.J. Slope movement types and processes. In *Schuster RL, Krizek RJ (eds) Landslides, Analysis and Control, Special Report 176: Transportation Research Board*; National Academy of Sciences: Washington, WA, USA, 1978; pp. 11–33.
28. Hungr, O.; Leroueil, S.; Picarelli, L. The Varnes classification of landslides types, an update. *Landslides* **2014,** *11*, 167–194, doi:10.10007/s10346-013-0436-y.
29. Pawłuszek, K.; Ziaja, M.; Borkowski, A. Accuracy assessment of the height component of the airborne laser scanning data collected in the ISOK system for the Widawa river valley. *Acta Sci. Polonorum Geod. Descr. Terr*. **2014**, *13*, 27–38. (In Polish).

30. Pourghasemi, H.R.; Pradhan, B.; Gokceoglu, C.; Mohammadi, M.; Moradi, H.R. Application of weights-of-evidence and certainty factor models and their comparison in landslide susceptibility mapping at Haraz watershed, Iran. *Arab. J. Geosci*. **2013**, *6*, 2351–2365, doi:10.1007/s12517-012-0532-7.
31. Pourghasemi, H.R.; Moradi, H.R.; Aghda, S.F.; Gokceoglu, C.; Pradhan, B. GIS-based landslide susceptibility mapping with probabilistic likelihood ratio and spatial multi-criteria evaluation models (North of Tehran, Iran). *Arab. J. Geosci.* **2014**, *7*, 1857–1878, doi:10.1007/s12517-012-0825-x.
32. Mashari, S.; Solaimani, K.; Omidvar, E. Landslide susceptibility mapping using multiple regression and GIS tools in Tajan Basin, North of Iran. *Environ. Nat. Resour. Res.* **2012**, *2*, 43, doi:10.5539/enrr.v2n3p43.
33. Penna, D.; Borga, M.; Aronica, G.T.; Brigandì, G.; Tarolli, P. Predictive power of a shallow landslide model in a high-resolution landscape: dissecting the effects of forest roads. *Hydrol. Earth Syst. Sci.* **2014**, *18*, 2127–2139, doi:10.5194/hess-18-2127-2014.
34. Sofia, G.; Tarolli, P. Automatic characterization of road networks under forest cover: advances in the analysis of roads and geomorphic process interaction. *Rend. Online Soci. Geol. Ital.* **2016**, *39*, 23–26, doi:10.3301/ROL.2016.38.
35. Tarolli, P.; Sofia, G. Human topographic signatures and derived geomorphic processes across landscapes. *Geomorphology* **2016**, *255*, 140–161, doi:10.1016/j.geomorph.2015.12.007.
36. Pawłuszek, K.; Borkowski, A. Automatic Landslides Mapping in the Principal Component Domain. In *Advancing Culture of Living with Landslides*; Mikoš, M., Vilímek, V., Yin, Y., Sassa, K., Eds.; WLF 2017; Springer: Cham, Switzerland, 2017; doi:10.1007/978-3-319-53483-1 50.
37. Chen, W.; Li, X.; Wang, Y.; Chen, G.; Liu, S. Forested landslide detection using LiDAR data and the random forest algorithm: A case study of the Three Gorges, China. *Remote Sens. Environ.* ***2014***, *152*, 291–301, doi:2010.1016/j.rse.2014.07.004.
38. Meyer, D. *Support Vector Machines*; FH Technikum: Vienna, Austria, 2017.
39. Moosavi, V.; Talebi, A.; Shirmohammadi, B. Producing a landslide inventory map using pixel-based and object-oriented approaches optimized by Taguchi method. *Geomorphology* **2014**, *204*, 646–656, doi:10.1016/j.geomorph.2013.09.012.